

Role of atomic bonding for compound and glass formation in Ni-Si, Pd-Si, and Ni-B systems

K. Tanaka and T. Saito

Department of Metallurgical Engineering, Nagoya Institute of Technology, Showa-ku, Nagoya 466, Japan

K. Suzuki

The Research Institute for Iron, Steel, and Other Metals, Tohoku University, Sendai 980, Japan

R. Hasegawa

Corporate Research and Development Center, Allied Corporation, Morristown, New Jersey 07960

(Received 19 February 1985)

Valence electronic structures of crystalline compounds and glassy alloys of Ni silicides, Pd silicides, and Ni borides are studied by soft-x-ray spectroscopy over wide ranges of Si and B concentrations. The samples prepared include bulk compounds, glassy ribbons, and amorphous sputtered films. Silicon $K\beta$ emissions of Ni and Pd silicides generally consist of a prominent peak fixed at ≈ 4.5 and ≈ 5.8 eV below the Fermi level E_F , respectively, with a shoulder near E_F which grows and shifts toward lower energy with increasing Si concentration. The former is identified as due to Si p -like states forming Si $3p$ -Ni $3d$ or Si $3p$ -Pd $4d$ bonding states while the latter as due to the corresponding antibonding states. Ni L_3 and Pd L_3 emissions of these silicides indicate that Ni $3d$ and Pd $4d$ states lie between the above two states. These local electronic configurations are consistent with partial-density-of-states (PDOS) calculations performed by Bisi and Calandra. Similar electronic configurations are suggested for Ni borides from B $K\alpha$ and Ni L_3 emissions. Differences of emission spectra between compounds and glasses of similar compositions are rather small, but some enhancement of the contribution of antibonding states to the PDOS near E_F is suggested for certain glasses over that of the corresponding compounds. These features are discussed in connection with the compound stability and glass formability.

I. INTRODUCTION

Studies of transition-metal silicides and borides in the form of compounds or glassy alloys have made remarkable progress in recent years. This is based not only on their potential use in electrical and material engineering but also on their importance in revealing fundamental aspects such as atomic bonding in transition-metal-metalloid systems. Precise knowledge of the process of silicide formation at silicon-metal interfaces and the physical properties of the silicides formed is now prerequisite to developing semiconducting devices.^{1,2} Likewise, knowledge of the characteristics of borides contributes significantly to the improvement of electronic and magnetic materials.^{3,4} However, less is known about the electronic structures on which the formability and physical properties of these compounds and glasses are based. In this paper we report the electronic structures of compounds and glassy alloys of Ni-Si, Pd-Si, and Ni-B systems as revealed by soft-x-ray spectroscopy (SXS), and discuss the role of atomic bonding for the compound and glass formation.

A number of experimental⁵⁻¹⁷ and theoretical¹⁸⁻²² studies have been published, which deal with the electronic states in the above materials. Most of the experiments have employed x-ray or ultraviolet photoelectron spectroscopy (XPS or UPS) to elucidate the band structures below the Fermi level E_F . This method provides band spectra connected with the total densities of states composed of d bands from transition metals and $s-p$ bands from metal-

loids. However, owing to markedly different photoionization cross sections, the spectra are usually dominated by the d bands leaving the $s-p$ bands relatively ineffective.⁵ The latter are revealed only by making use of the Cooper minimum or resonant photoemission technique.¹² In contrast, the SXS method is capable of extracting information about the partial densities of states (PDOS) associated with each constituent, which may enable us to identify the transition-metal d bands and the metalloid $s-p$ bands as well as their hybridized states more definitely than employing XPS or UPS method.

In this study, Si $K\beta$ and B $K\alpha$ emissions were measured which reflect the PDOS of Si and B p -like states, respectively, and were compared with Ni L_3 and Pd L_3 emissions projecting the PDOS of Ni and Pd d -like states, respectively, in the above compounds and glassy alloys. One of the disadvantages inherent in using the SXS method to study valence-band structures arises from the fact that Fermi edges cannot always be clearly defined particularly for the transition-metal L_3 emissions. This difficulty, however, could be removed by measuring self-absorption spectra corresponding to the Ni L_3 and Pd L_3 absorptions simultaneously.

II. EXPERIMENTAL

A. Sample preparation

Several kinds of bulk silicides and borides were prepared for Ni-Si, Pd-Si, and Ni-B systems. The starting

materials used were 99.99%-pure Ni, 99.99%-pure Pd, 99.999%-pure Si, and 99.8%-pure B. Appropriate amounts of the raw materials were melted together either by induction heating in vacuum using high-purity alumina crucibles or by arc melting in a copper hearth under a high-purity argon-gas atmosphere at 1 atm. The disk-shaped samples thus prepared were homogenized at high temperatures, spark cut into pieces, and subjected to x-ray-diffraction analysis. It was confirmed that they were composed of single phases except for NiSi₂ and Pd₃Si which contained minor quantities of secondary phases. The Ni₄B₃ compound exhibited a mixture of orthorhombic and monoclinic phases. The compounds prepared, their crystal structures²³⁻²⁶ and the heat treatments employed are listed in Table I.

Glassy alloys were prepared either by liquid quenching (Pd-Si and Ni-B) or by rf sputtering (Ni-Si). Liquid quenching was performed using a single roll in a vacuum or under reduced argon-gas pressures. Ribbon samples thus prepared were $\approx 20 \mu\text{m}$ thick and 1-5 mm wide. Their x-ray diffraction patterns showed halos indicative of glassy structures. Only the pattern of Pd₇₅Si₂₅ included small additional crystalline peaks. The rf sputtering was carried out under an argon-gas pressure of 5×10^{-3} Torr with a combination of a Si wafer and a Ni plate as a tar-

get and an electrolytically polished Al plate as a substrate. Alloy films of $\approx 1 \mu\text{m}$ in thickness were produced and their Si contents were determined by x-ray microanalysis. Amorphous phases were formed for the compositions Ni₆₃Si₃₇ and Ni₄₇Si₅₃. For lower Si contents, crystalline and amorphous phases coexisted. The glassy alloys prepared are also listed in Table I. All the bulk and ribbon samples were mechanically polished before the SXS measurements until clean and optically flat surfaces were obtained. The sputtered films were measured without any further treatments.

B. SXS measurements

Soft x-ray emissions were measured using an x-ray microanalyzer of a conventional style described elsewhere.²⁷⁻²⁹ An electron beam of 10 keV and $\approx 10 \mu\text{A}$ with a diameter of 50 μm was usually employed as the source for excitation, and its angle of incidence was normal to the sample surface. X-rays emitted at an angle of 38.5° from the surface were monochromatized by a Johannson-type crystal with a radius of curvature of 250 mm and detected by a gas-flow proportional counter after passing through a slit of 0.1 mm. A pentaerythritol crystal ($2d=8.75 \text{ \AA}$) was used as the dispersing crystal for Si $K\beta$ ($\lambda=6.75 \text{ \AA}$) and Pd L_3 ($\lambda=3.91 \text{ \AA}$) emissions; for the latter, second-order reflection was utilized to improve the resolution. For Ni L_3 ($\lambda=14.6 \text{ \AA}$) and B $K\alpha$ ($\lambda=67.6 \text{ \AA}$) emissions, potassium acid phthalate ($2d=26.4 \text{ \AA}$) and Pb stearate ($2d=100.2 \text{ \AA}$) crystals were used, respectively. The spectral resolution (core-level width plus instrumental width) was estimated to be $\approx 0.8-0.9 \text{ eV}$ for B $K\alpha$ and Si $K\beta$, $\approx 1.0 \text{ eV}$ for Ni L_3 , and $> 1.5 \text{ eV}$ for Pd L_3 emissions. Samples were continuously shifted with respect to the electron beam during the measurements, which proved to be quite effective in minimizing the effect of contamination. The spectrum of each sample was measured repeatedly until the reproducibility was satisfactory.

III. RESULTS

Figure 1 shows Si $K\beta$ emissions of a series of bulk compounds and amorphous alloy films (denoted by a prefix *a*) of Ni-silicides together with a supersaturated crystalline alloy, *c*-Ni₈₂Si₁₈, arranged in order of increasing Si concentration. Each spectrum is normalized to the maximum intensity and plotted against photon energy. It can be seen from the figure that these spectra are characterized by three features, i.e., shoulder *A* near the emission edge, central peak *B*, and its substructure *B'* at a lower energy. Although the peak position ($1835.5 \pm 0.2 \text{ eV}$) is very close to that of pure Si (1835.9 eV), structures corresponding to *A* and *B'* are not seen in the latter.²⁶ The shoulder *A* becomes well defined with increasing Si content and tends to move toward lower energy in NiSi and NiSi₂. The substructure *B'* is seen most clearly in Ni₃Si, but becomes less evident in the materials with higher Si contents. Differences between the profiles of compound and amorphous samples of similar concentrations are rather small. Their comparisons are made in the next section.

TABLE I. List of the samples prepared, their crystal structures, and heat treatments. WQ denotes water-quenched samples, FC furnace-cooled samples.

Samples	Crystal structures	Heat treatments
<i>c</i> -Ni ₈₂ Si ₁₈	fcc Ni(α)+(β phase)	1130 °C 3 h, WQ
Ni ₃ Si	fcc <i>L</i> ₁ (Cu ₃ Au type)	1000 °C 24 h, FC
Ni ₂ Si	orthorhombic <i>C</i> ₂₃ (PbCl ₂ type)	1000 °C 24 h, FC
NiSi	orthorhombic <i>B</i> ₃₁ (MnP type)	900 °C 24 h, FC
NiSi ₂	fcc <i>C</i> ₁ (CaF ₂ type)	900 °C 24 h, FC
<i>a</i> -Ni ₆₃ Si ₃₇	amorphous	
<i>a</i> -Ni ₄₇ Si ₅₃	amorphous	
Pd ₃ Si	orthorhombic <i>D</i> ₀₁₁ (Fe ₃ C type)	900 °C 5 h, FC
Pd ₂ Si	hexagonal <i>C</i> ₂₂ (Fe ₂ P type)	no treatment
PdSi	orthorhombic <i>B</i> ₃₁ (MnP type)	no treatment
<i>a</i> -Pd ₈₅ Si ₁₅	amorphous	
<i>a</i> -Pd ₈₃ Si ₁₇	amorphous	
<i>a</i> -Pd ₈₀ Si ₂₀	amorphous	
<i>a</i> -Pd ₇₈ Si ₂₂	amorphous	
<i>a</i> -Pd ₇₅ Si ₂₅	amorphous+(Pd ₃ Si)	
Ni ₃ B	orthorhombic <i>D</i> ₀₁₁ (Fe ₃ C type)	850 °C 50 h, FC
Ni ₂ B	bct <i>C</i> ₁₆ (CuAl ₂ type)	800 °C 24 h, FC
Ni ₄ B ₃	orthorhombic + monoclinic	850 °C 24 h, FC
NiB	orthorhombic <i>B</i> _{<i>f</i>} (ζ CrB type)	800 °C 24 h, FC
<i>a</i> -Ni ₇₅ B ₂₅	amorphous	
<i>a</i> -Ni ₆₇ B ₃₃	amorphous	
<i>a</i> -Ni ₆₁ B ₃₉	amorphous	

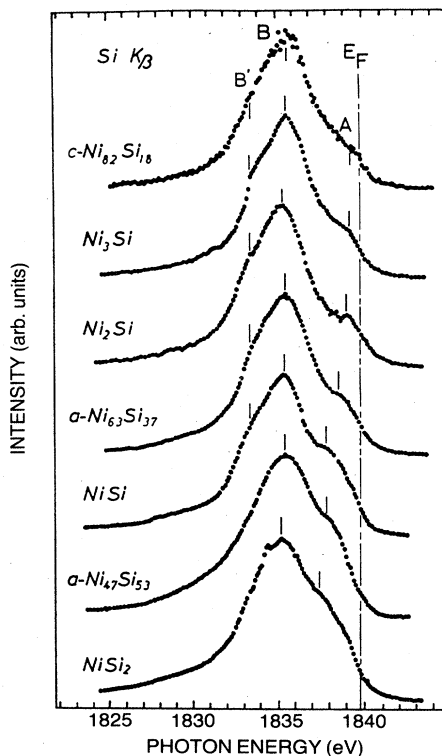


FIG. 1. Si $K\beta$ emission spectra for a solid solution, crystalline compounds and amorphous alloys of the Ni-Si system arranged in the order of Si concentration. Features *A*, *B*, and *B'* are indicated by vertical bars.

Determination of the Fermi edges of these spectra is not straightforward, but they may commonly be taken to be just above the shoulder *A*, i.e., the half-height position (1839.8 eV) of the steep descent, as shown in the figure. This photon energy was chosen as the Fermi level for all the Ni silicides as well as for the Pd silicides (Fig. 4); this choice is based on the empirical fact that, in many non-transition-metal-transition-metal (or noble-metal) systems, the photon energy corresponding to the Fermi edge of the $K\beta$ emission of a nontransition metal is kept almost fixed despite the wide changes of alloying species and alloy compositions.^{30,31}

Figure 2 shows the Ni L_3 emissions of pure Ni and several compounds of Ni silicides whose intensities are normalized to the respective peak heights. Two accelerating voltages, 5 and 20 kV, are employed for this measurement. The L_3 emission undergoes some peak shift for the two excitations; the shift is the largest in pure Ni and the smallest in NiSi and NiSi₂, the latter manifesting deviations of the emission intensity only around the high-energy tails of the spectra. The large peak shift of pure Ni is associated with the strong self-absorption at the L_3 absorption edge.^{32,33} The degree of the self-absorption may be evaluated by the ratio of the two emission intensities, $I_{5\text{kV}}/I_{20\text{kV}}$, as shown by the solid curve of arbitrary scale for each sample. In pure Ni and Ni₃Si, the ratio

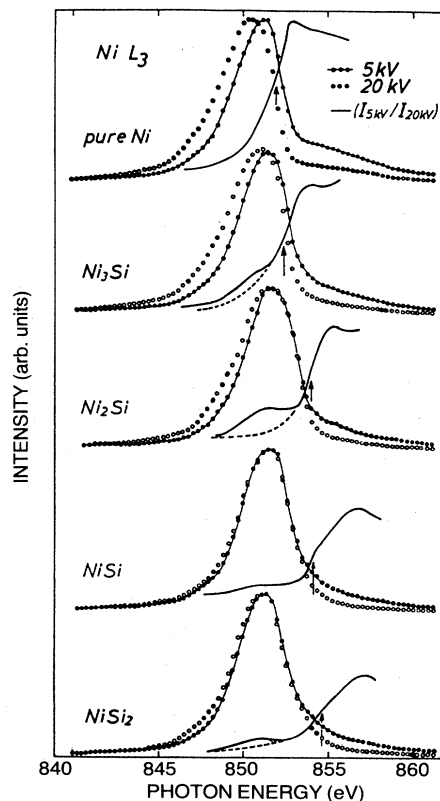


FIG. 2. Ni L_3 emission spectra for pure Ni and crystalline compounds of the Ni-Si system measured at 5- and 20-kV excitations. Solid curves show self-absorptions of Ni defined by the ratios of emission intensities corresponding to the two accelerating voltages. Absorption edges are indicated by arrows.

rises sharply at photon energies just above the emission peaks of the 5-kV excitation, while in the other compounds it tends to rise at higher energies with smaller amplitudes. The photon energy corresponding to the steepest increase of the self-absorption curve is defined here as the L_3 absorption edge of Ni in the sample (shown by the arrow for each curve), which is supposed to agree approximately with the Fermi cutoff energy of the corresponding L_3 emission. The Ni L_3 emission spectra of 5 kV excitation against energy relative to the Fermi level thus defined are shown in Fig. 3. It can be seen that the emission peak representing Ni d band is located just below E_F in pure Ni but is shifted by ≈ 1.0 , ≈ 2.4 , ≈ 2.7 , and ≈ 3.3 eV toward lower energy in Ni₃Si, Ni₂Si, NiSi, and NiSi₂, respectively, with a concomitant variation of the emission profile. These features are generally consistent with those observed in the UPS study of Franciosi *et al.*¹⁰ The downward shift of the L_3 peak with respect to the Fermi level is associated with the filling of the d band upon silicide formation, and results in a marked decrease of the intensity at E_F .

Figure 4 shows Si $K\beta$ emissions of glassy alloys and compounds of Pd silicides arranged in the order of increasing Si content. Like the Ni silicides, the spectra are composed of shoulders (*A*) and prominent peaks (*B*). As

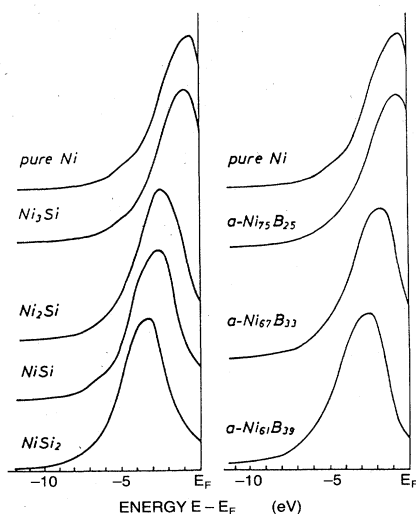


FIG. 3. Ni L_3 emission spectra below E_F for pure Ni, crystalline Ni-Si compounds and Ni-B glassy alloys, whose Fermi levels line up at the energy zero.

the Si concentration increases from 15 at. % to 25 at. % in the glassy alloys, the shoulder *A* grows to form a clear peak. This peak becomes clearer but moves slightly toward lower energy in Pd_2Si ; further peak growth and

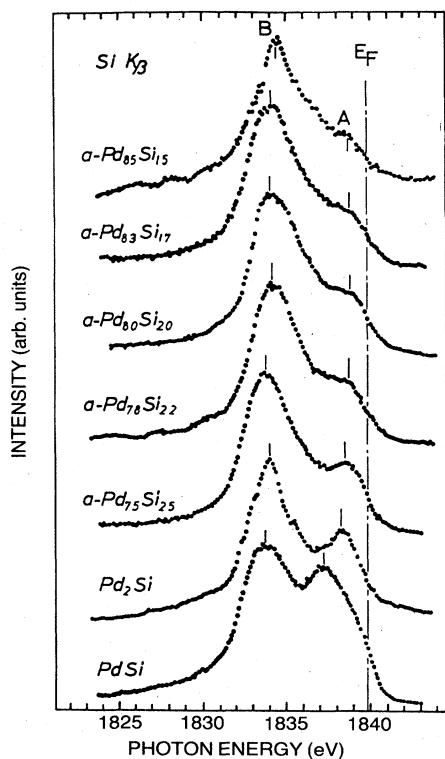


FIG. 4. Si $K\beta$ emission spectra for glassy alloys and crystalline compounds of Pd-Si system arranged in the order of Si concentration. Features *A* and *B* are indicated by vertical bars.

downward shift take place in PdSi . On the other hand, the peak *B* is fixed at 1834.0 ± 0.3 eV in all the glasses and compounds, which is narrower and ≈ 1.5 eV lower than the corresponding peak in the Ni silicides. Pd L_3 emissions of some of these samples were measured and their Fermi cutoff energies were determined by the self-absorption technique described above. The spectra were compared with the Si $K\beta$ counteremissions (Fig. 7).

Figure 5 shows B $K\alpha$ emissions of several glassy alloys and compounds of Ni borides presented in the order of B concentration. All these spectra are, like the Si $K\beta$ emissions presented thus far, characterized by the shoulder *A* near the emission edge and the central peak *B* fixed at 182.5 ± 0.2 eV. This energy is only slightly lower than the peak energy (183.3 eV) for pure crystalline B; nevertheless, the overall spectral features are very different from those of pure B.²⁷ One notable feature of the B $K\alpha$ spectra in comparison with the Si $K\beta$ spectra is that the shoulder *A* varies very little despite the wide change of B concentration, except for Ni_2B which exhibits an anomalously small shoulder. The Fermi level may commonly be taken at 187.0 eV, as shown in the figure. The peak *B* is thus situated at ≈ 4.5 eV below E_F , which is comparable with the depth (≈ 4.3 eV) of the corresponding peak in the Ni silicides.

Ni L_3 emissions of these borides were measured and their Fermi edges were determined in the same way as for the Ni silicides. The spectra for the glassy alloys are

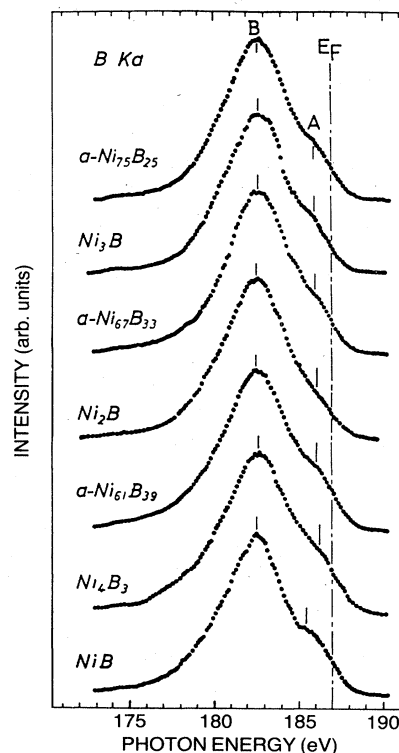


FIG. 5. B $K\alpha$ emission spectra for glassy alloys and crystalline compounds of Ni-B system arranged in the order of B concentration. Features *A* and *B* are indicated by vertical bars.

shown in Fig. 3. It can be seen that the emission peak shifts toward lower energy with increasing B concentration; it is located at ≈ 0.6 , ≈ 1.6 , and ≈ 2.3 eV below E_F for 25 at. %, 33 at. %, and 39 at. % B, respectively. This behavior is similar to the result for the Ni silicides.

IV. DISCUSSION

A. Local electronic structures revealed by the SXS results

The present SXS data indicate that the electronic structures of transition metals and metalloids undergo certain modifications upon compound or glass formation. This may reasonably be accounted for by taking into consideration the effect of atomic bonding between the transition metals and metalloids. The first experimental verification of the atomic bonding was made by Riley *et al.*⁵ for α -Pd₈₁Si₁₉ by combining Auger electron spectroscopy (AES), XPS, and UPS techniques. They constructed PDOS curves for Pd d and Si s - p electrons, and emphasized the importance of covalentlike bonding between Pd d and Si p states. A similar study was performed for Pd₂Si by Ho *et al.*,¹⁶ who measured UPS and AES spectra for the silicide and interpreted the data based on the calculated PDOS of artificial Pd₃Si and PdSi crystals. They found that Pd $4d$ states interact strongly with Si $3p$ states. The resulting p - d hybrid complex is composed of nonbonding d states of Pd lying at ≈ 2.8 eV below E_F and two other states separated by ≈ 5 eV; the lower-lying states form Si $3p$ -Pd $4d$ bonding states, while the higher-lying states near E_F form the corresponding antibonding states. Similar results have been reported for the Pd silicides formed at the Pd/Si film interface.¹⁷ The above works were followed by a more elaborate and systematic study by Bisi and Calandra¹⁸ who carried out linear-combination-of-atomic-orbitals band calculations for Ni, Pd, and Pt silicides without modifying their real crystal structures. In the following, we discuss local electronic structures in Ni and Pd silicides and Ni borides based on our SXS results and Bisi and Calandra's calculations.

1. Ni silicides

In Fig. 6, Ni L_3 and Si $K\beta$ emissions of Ni₂Si, NiSi, and NiSi₂ are compared where the Fermi levels lie at the origin of the common energy axis. The intensity of the Si $K\beta$ emission relative to the Ni L_3 emission is appropriately reduced so as to facilitate the comparison. The PDOS curves for Ni d and Si s - p states¹⁸ are also shown for each silicide in an arbitrary scale in the figure. It can be seen for all the silicides that the Ni L_3 peaks fall between the shoulders A and the peaks B of the Si $K\beta$ spectra. In addition, the lower-energy portions of the Ni L_3 peaks somewhat bulge out where the structures B and B' of the Si $K\beta$ spectra are seen.

These features can be interpreted in terms of the calculated PDOS. The structures B and B' located at -4.5 and -6.5 eV, respectively, in Ni₂Si and Ni₃Si (Fig. 1) represent the Si p states which hybridize with the Ni d states forming p - d bonding states, while the structure A near E_F comes from the similar states contributing to p - d antibonding states which are split off from the bonding

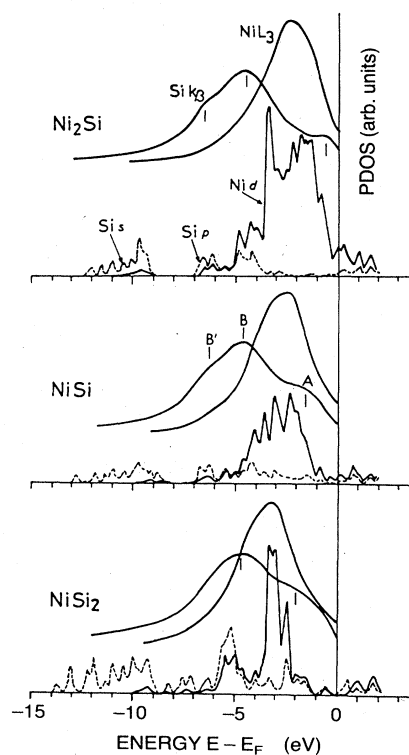


FIG. 6. Comparison of Si $K\beta$ and Ni L_3 emission spectra with calculated PDOS curves (Ref. 18) for crystalline compounds Ni₂Si, NiSi, and NiSi₂.

states to above the nonbonding Ni d states; the tail portion of the antibonding states filled with electrons actually causes the structure A . These antibonding states are partly pulled down to below E_F in the higher silicides, and cause the shoulder A to grow and move toward lower energy, i.e., -1.5 and -2.0 eV in NiSi and NiSi₂, respectively. A reduced Ni-Si interaction may explain the above effect.¹⁸ In contrast, in c -Ni₈₂Si₁₈, the shoulder A is small and lies just below E_F (Fig. 1); it practically disappears in c -Ni₉₁Si₉.³⁰ In these alloys with low Si concentrations, the antibonding states are pushed up well above E_F and hence have a small PDOS at E_F .

On the other hand, the Ni L_3 peak is dominated by the nonbonding Ni d states, whose centroid shifts from ≈ -2 eV in Ni₂Si to ≈ -3 eV in NiSi₂ with some narrowing of the width (Figs. 3 and 6). Thus, the overall spectral features of the Si $K\beta$ and Ni L_3 emissions are consistent with the PDOS results. As a consequence of the selection rules, information on the Si s -like states is not available from the present SXS data. However, as shown by calculations,¹⁸⁻²² these states (≈ -10 eV) lie far below the Ni d states and hence would make only a minor contribution to the atomic bonding.

2. Pd silicides

A comparison of the Si $K\beta$ and Pd L_3 emission with the calculated PDOS curves¹⁸ are made in Fig. 7 for Pd₂Si

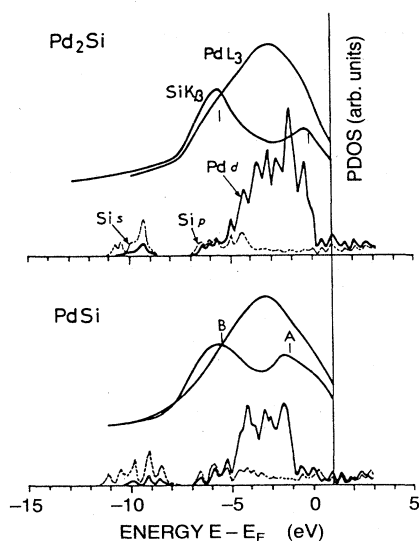


FIG. 7. Comparison of Si $K\beta$ and Pd L_3 emission spectra with calculated PDOS curves (Ref. 18) crystalline compounds Pd_2Si and PdSi .

and PdSi . The Si $K\beta$ emission consists of two well-resolved peaks whose separation is ≈ 4.6 and ≈ 3.5 eV in Pd_2Si and PdSi , respectively; the peak B is fixed at -5.8 eV while the peak A moves from -1.2 eV in Pd_2Si to -2.3 eV in PdSi . The Pd L_3 emission is broader than the corresponding Ni L_3 emission shown above reflecting Pd $4d$ bands being wider than Ni $3d$ bands. However, its peak is seen to fall between the two Si $K\beta$ emission peaks in both silicides. These features are, in general, consistent with the calculated PDOS.

The peak B of the $K\beta$ emission is identified as Si p states which combine with Pd d states to form $p-d$ bonding states at the bottom if nonbonding Pd d states, while the peak A corresponds to the antibonding states formed above the nonbonding d states. The energy levels of these antibonding states are considered to change with Si content similarly to those in the Ni silicides described above. Thus, the variation of the structure A with Si concentration in the glasses and compounds shown in Fig. 4 can be explained as follows. The antibonding states existing above E_F in low concentrations ($< \sim 15$ at. % Si) are progressively lowered in energy with increasing Si concentration, passing across E_F around ≈ 20 – 25 at. % Si, and pulled down to below E_F at higher concentrations (Pd_2Si and PdSi). This progressive downward shift of antibonding states should cause a maximum of PDOS at E_F when they straddle the Fermi level. Indeed, a very clear shoulder with strongest relative intensity is observed in the glassy alloy with 20 at. % or 22 at. % Si (see Fig. 4). This behavior is consistent with the low-temperature specific-heat data for Pd-Si-(Cu) glassy alloys of Mizutani *et al.*,³⁴ which suggest the presence of a small density-of-states maximum between 16.5 at. % and 22 at. % Si. The formation of $p-d$ bonding states has already been confirmed

for Pd_2Si by UPS studies,^{12,16} while the above nature of antibonding states, which generally agrees well with band calculations,^{16,18} has been revealed for the first time by the present SXS study.

3. Ni borides

As shown in Fig. 5, the B $K\alpha$ emission consists of peak B at ≈ -4.3 eV from E_F and clear shoulder A near E_F . On the basis of the above discussion, it seems reasonable to attribute the peak B to bonding states involving B $2p$ and Ni $3d$ states, whereas the shoulder A corresponds to the corresponding antibonding states cutoff at E_F . However, the profile change of the shoulder A with the boron content is not so significant as that of the Si $K\beta$ emission; it is more or less fixed near E_F and has a similar intensity for a wide range of composition except for Ni_2B which has a much smaller shoulder than the others. These features may suggest that the antibonding states in Ni-borides are structure dependent rather than concentration dependent. Panissod *et al.*³⁵ have shown by NMR measurements that in Ni-B glassy alloys the local environment about a boron atom is an admixture of Ni_3B - and Ni_4B_3 -type structures (nickel trigonal prisms) which differ from that of Ni_2B (nickel anticubes). A similar result has been obtained by Suzuki *et al.*³⁶ through neutron scattering experiments. A boron atom has 5.2–6 nickel neighbors in Ni_3B - and Ni_4B_3 -type structures, whereas it has 8 neighbors in Ni_2B , the Ni-B separation being almost conserved (2.11 ± 0.03 Å).³⁶ Nickel-boron interactions are therefore expected to be weaker in the former than in the latter. This may cause the antibonding states to stay around the Fermi level giving rise to a definite shoulder in the former, while they are pushed up above the Fermi level resulting in a smaller shoulder in the latter. However, no reliable band calculations have been performed for Ni borides to compare with the present SXS data confirming the present interpretation.

B. Characteristics of the electronic structures in glassy alloys

We have discussed thus far, certain features of the local electronic structures in silicides and borides without specifying their crystalline or glassy structures. In this section we briefly examine if any differences are observed in the SXS spectra between the two kinds of alloy phases. Since the emission spectra vary more or less with composition, such a test be made for compounds and glassy alloys with identical or at least comparable metalloid concentrations.

Figure 8 shows Si $K\beta$ and B $K\alpha$ emissions of certain silicides and borides in crystalline (dashed curves) and glassy (solid curves) states. It can be seen from the figure that the spectra of the compound and the glass of any composition are mutually quite similar, except that the shoulder around E_F is somewhat more intense in the glass than in the compound (the spectra for $a\text{-Ni}_{61}\text{B}_{39}$ and Ni_4B_3 almost coincide with each other). This feature may suggest that the contribution of the bonding states to the PDOS of the metalloid changes little between the two states, but that of the antibonding states is more enhanced in the glass than in the compound. It is not clear whether

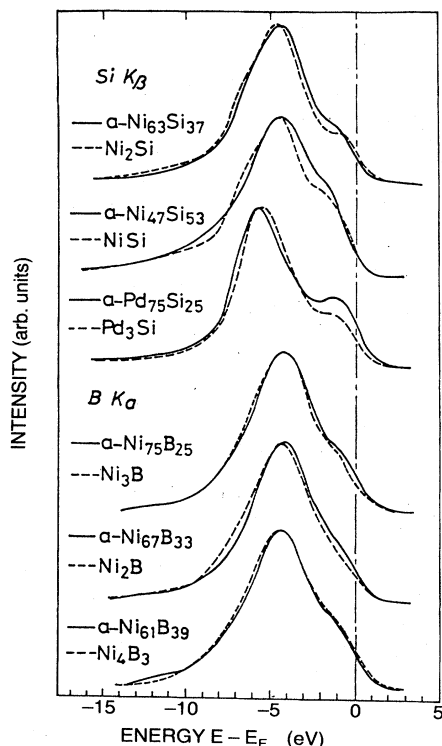


FIG. 8. Comparison of Si $K\beta$ and B $K\alpha$ emission spectra between glassy alloys (solid curves) and crystalline compounds (dashed curves) with similar concentrations for Ni-Si, Pd-Si, and Ni-B systems.

this enhancement occurs as a result of the difference in local atomic environments, or if it comes from the lack of long-range order in glassy structures.³⁷ However, this seems to be reasonable in view of the fact that the total electronic energy of a glass should perhaps be higher than that of the crystalline counterpart.

Assuming constant transition probabilities for p electrons of Si and B, a rough estimate is made of the energy gain per metalloid p electron of a glass relative to its compound by evaluating the difference of the centroids of the two spectra. This yields $\Delta\epsilon$ (eV) ≈ 0.2 (α -Ni₆₃Si₃₇ and α -Ni₆₇B₃₃), ≈ 0.1 (α -Pd₇₅Si₂₅ and α -Ni₇₅B₂₅), and $\Delta\epsilon < 0.05$ (α -Ni₄₇Si₅₃ and α -Ni₆₁B₃₉).³⁸ Now, assuming two $3p$ electrons per Si atom contribute to the p - d bonding in the silicides, the total energy gain of Si $3p$ electrons in, e.g., α -Pd₇₅Si₂₅ is calculated as

$$\Delta E \approx 0.1 \times 2 \times 0.25 = 0.05 \text{ eV}/(\text{Pd} + \text{Si atom})$$

or

$$\Delta E \approx 1 \text{ kcal/mol.}$$

This value is comparable with the heat evolved upon crystallization in α -(Pd_{92.8}Cu_{7.2})_{100-x}Si_x ($15.5 \leq x \leq 20.5$) and α -(Pd_{82.4}Si_{17.6})_{100-y}Cu_y ($0 \leq y \leq 14$) measured by calorimetry.³⁹ For a more precise estimation of ΔE , we must take into account the effects of other electrons, of which d electrons would be most important. However, as

shown in Figs. 3, 6, and 7, the d bands of Ni and Pd tend to be filled, shifted downward, and narrowed for metalloid concentrations exceeding ≈ 25 at. %. In these cases, the difference in the atomic arrangements would not alter the d -band structure considerably. Further experimental and theoretical studies are necessary to elucidate these points.

C. Effect of atomic bonding on the compound stability and glass formability

Atomic bonding between transition metals and metalloids manifests two opposing aspects upon compound and glass formation.^{40,41} Firstly, it stabilizes a compound by forming bonding states and thereby reducing the energy of valence electrons. Secondly, it destabilizes the compound through the corresponding antibonding states when they are filled. The experimental data given above seem to clarify these points further, leading to the following general statements. In Ni and Pd whose d bands are almost full, addition of elements such as Si and B causes their Fermi levels to be lifted up above the d bands and the antibonding states to be partially filled. In certain ranges of metalloid concentrations, the Fermi level lie near the centroids of the antibonding states, where the stability of compounds would be lost to some extent. In such conditions, the energy differences between the compounds and the corresponding glassy alloys would also decrease, resulting in increased tendency to glass formation. At higher metalloid concentrations, the Fermi levels lie well above the centroids of the antibonding states, which restores the stability of compounds leading to decrease in the glass formability. The present interpretation for the glass formability is based on the experimental observation that the glassy structures can be formed in the silicides and borides only in the restricted ranges of metalloid concentrations where the metalloid $K\beta$ emissions manifest definite shoulders just below the Fermi levels. This picture of the correlation between compound stability and glass formability appears to be valid for the above transition-metal silicides and borides whose d bands are entirely filled. For other silicides and borides such as Cr₃Si, Fe₃B, and Co₃B, the situation would inevitably be more complicated because in these materials the d bands are not entirely filled and may make a dominant contribution to the compound and/or glass formation.

V. CONCLUSION

It is shown that soft-x-ray spectroscopy provides information about the local electronic density of states for transition-metal silicides and borides in glassy and crystalline states. When combined with the diffraction data and band calculations, these local electronic configurations reveal the importance of the antibonding states in understanding the roles of atomic bonding in compound and glass formation in transition-metal-metalloid systems.

ACKNOWLEDGMENT

The authors are grateful to Dr. K. Masui for his collaboration in preparing amorphous sputtered films of Ni silicides.

- ¹See papers in *Thin-Film Interdiffusion and Reactions*, edited by J. M. Poate, K. N. Tu, and J. W. Mayer (Wiley, New York, 1978), p. 359.
- ²See papers in Proceedings of the Seventh Annual Conference on the Physics of Compound Semiconductor Interfaces [J. Vac. Sci. Technol. **17**, 869 (1980)].
- ³F. E. Luborsky, in *Ferromagnetic Materials*, edited by E. P. Wohlfarth (North-Holland, Amsterdam, 1980), Vol. 1, p. 451.
- ⁴See papers in *Amorphous Metallic Alloys*, edited by F. E. Luborsky (Butterworths, London, 1983), Chaps. 14–23.
- ⁵J. D. Riley, L. Ley, J. Azoulay, and K. Terakura, Phys. Rev. B **20**, 776 (1979).
- ⁶P. Oelhafen, M. Liad, H.-J. Güntherodt, K. Berresheim, and H. D. Polaschegg, Solid State Commun. **30**, 641 (1979).
- ⁷B. J. Wacławski and D. S. Boudreaux, Solid State Commun. **33**, 589 (1980).
- ⁸P. J. Grunthaner, F. J. Grunthaner, A. Madhukar, and J. W. Mayer, J. Vac. Sci. Technol. **19**, 649 (1981).
- ⁹P. J. Grunthaner, F. J. Grunthaner, and A. Madhukar, J. Vac. Sci. Technol. **20**, 680 (1982).
- ¹⁰A. Franciosi, J. H. Weaver, and F. A. Schmidt, Phys. Rev. B **26**, 546 (1982).
- ¹¹Yu-Jeng Chang and J. L. Erskine, Phys. Rev. B **26**, 7031 (1982).
- ¹²A. Franciosi and J. H. Weaver, Phys. Rev. B **27**, 3554 (1983).
- ¹³Y. Shiraki, K. L. I. Kobayashi, H. Daimon, A. Ishizuka, S. Sugai, and Y. Murata, Physica **117&118B**, 843 (1983).
- ¹⁴T. Honda, F. Itoh, and K. Suzuki, in *Proceedings of the Fourth International Conference on Rapidly Quenched Metals, Sendai, 1981*, edited by T. Masumoto and K. Suzuki (Japan Institute of Metals, Sendai, 1982), p. 1303.
- ¹⁵J. H. Weaver, A. Franciosi, and V. L. Moruzzi, Phys. Rev. B **29**, 3293 (1984).
- ¹⁶P. S. Ho, G. W. Rubloff, J. E. Lewis, V. L. Moruzzi, and A. R. Williams, Phys. Rev. B **22**, 4784 (1980).
- ¹⁷G. Rossi, I. Abbati, L. Braicovich, I. Lindau, and W. E. Spicer, Solid State Commun. **39**, 195 (1981).
- ¹⁸O. Bisi and C. Calandra, J. Phys. C **14**, 5479 (1981).
- ¹⁹D. M. Bylander, L. Kleinman, and K. Mednick, Phys. Rev. B **25**, 1090 (1982).
- ²⁰Y. J. Chabal, D. R. Hamann, J. E. Rowe, and M. Schluter, Phys. Rev. B **25**, 7598 (1982).
- ²¹D. M. Bylander, L. Kleinman, K. Mednick, and W. R. Grise, Phys. Rev. B **26**, 6379 (1982).
- ²²J. Tersoff and D. R. Hamann, Phys. Rev. B **28**, 1168 (1983).
- ²³M. Hansen and K. Anderko, *Constitution of Binary Alloys* (McGraw-Hill, New York, 1958).
- ²⁴R. P. Elliott, *Constitution of Binary Alloys*, 1st suppl. (McGraw-Hill, New York, 1965).
- ²⁵W. B. Pearson, *Handbook of Lattice Spacing and Structures of Metals and Alloys* (Pergamon, New York, 1958).
- ²⁶*Metals Reference Book*, 5th ed., edited by C. J. Smithells (Butterworths, London, 1976).
- ²⁷K. Tanaka, M. Yoshino, and K. Suzuki, J. Phys. Soc. Jpn. **51**, 3882 (1982).
- ²⁸K. Tanaka, T. Saito, and M. Yasuda, J. Phys. Soc. Jpn. **52**, 1718 (1983).
- ²⁹K. Tanaka, Y. Yamada, K. Kai, and K. Suzuki, J. Phys. Soc. Jpn. **53**, 1783 (1984).
- ³⁰K. Tanaka, M. Matsumoto, S. Maruno, and A. Hiraki, Appl. Phys. Lett. **27**, 529 (1975).
- ³¹K. Tanaka and A. Hiraki, Proceedings of the International Conference on X-Ray and X-Ray Ultraviolet Spectroscopy, Sendai, 1978, edited by T. Sagawa [Jpn. J. Appl. Phys. Suppl. **17**, 121 (1978)].
- ³²R. J. Liefeld, in *Soft X-Ray Band Spectra*, edited by D. J. Fabian (Academic, London, 1969), p. 133.
- ³³R. S. Crisp, J. Phys. F **13**, 1325 (1983).
- ³⁴U. Mizutani, K. T. Hartwig, T. B. Massalski, and R. W. Hopper, Phys. Rev. Lett. **41**, 661 (1978).
- ³⁵P. Panissod, I. Bakonyi, and R. Hasegawa, Phys. Rev. B **28**, 2374 (1983).
- ³⁶K. Suzuki, T. Fukunaga, F. Itoh, and N. Watanabe, in *Proceedings of the Fifth International Conference on Rapidly Quenched Metals*, Würzburg, 1984, edited by S. Steeb and H. Warlimont (North-Holland, Amsterdam, 1985), p. 479.
- ³⁷V. L. Moruzzi, P. Oelhafen, and A. R. Williams, Phys. Rev. B **27**, 7194 (1983).
- ³⁸Although absolute values estimated for E_F may have accuracies within 0.1 eV for Si $K\beta$ and B $K\alpha$ emissions, their relative values are accurate to within about 0.05 eV. This is valid especially for the cases in which glassy and crystalline materials with the same chemical compositions are compared.
- ³⁹H. S. Chen and B. K. Park, Acta Metall. **21**, 395 (1973).
- ⁴⁰C. D. Gelatt, Jr., A. R. Williams, and V. L. Moruzzi, Phys. Rev. B **27**, 2005 (1983).
- ⁴¹A. R. Williams, C. D. Gelatt, Jr., W. D. Connolly, and V. L. Moruzzi, in *Alloy Phase Diagrams*, edited by L. H. Bennett, T. B. Massalski, and B. C. Giessen (North-Holland, New York, 1983), p. 17.